Applied Nanoscience (2020) 10:2489–2494
https://doi.org/10.1007/s13204-019-01081-7

ORIGINAL ARTICLE

Electrical properties of *n*-HgCdTe MIS structures with HgTe single quantum wells

I. I. Izhnin[1] · I. I. Syvorotka[1] · A. V. Voitsekhovskii[2] · S. N. Nesmelov[2] · S. M. Dzyadukh[2] · S. A. Dvoretsky[2,3] · N. N. Mikhailov[3]

Received: 12 November 2018 / Accepted: 10 June 2019 / Published online: 17 June 2019
© King Abdulaziz City for Science and Technology 2019

Abstract
For the first time, the electrical characteristics of the metal–insulator–semiconductor (MIS) structures based on $n(p)$-$Hg_{1-x}Cd_xTe$ grown by molecular beam epitaxy including HgTe single quantum well (SQW) with thickness of 6.5 nm were investigated. SQW significantly influences the voltage, frequency, and temperature dependencies of the admittance of the MIS structure. When the SQW thickness is less than the critical thickness, there are numerous sharp maxima in the capacitance–voltage (C–V) curve, and when the thickness of the well is close to the critical thickness, a wide maximum is observed in the C–V characteristics associated with overshoot of minority charge carriers from SQW. A distinction is revealed between the effect of radiation on capacitive maxima caused by the escape of charge carriers from SQW and the recharging of deep levels in the epitaxial film bulk.

Keywords Single quantum well · Molecular beam epitaxy · Metal–insulator–semiconductor structure · Admittance · Capacitance–voltage characteristic

Background

The narrow-gap semiconductor solid solution $Hg_{1-x}Cd_xTe$ is widely used to create highly sensitive infrared focal plane arrays for different spectral ranges. The method of molecular beam epitaxy (MBE) of HgCdTe provides an ability to control the distribution of composition and impurity dopant along the thickness of the epitaxial film. Due to its high spatial resolution, this method is well suited for growing low-dimensional structures based on HgCdTe with quantum wells and superlattices. Low-dimensional structures are promising for the creation of new types of infrared detectors (Selamet et al. 2004; Benyahia et al. 2016; Dvoretsky et al. 2010), but, so far, the level of development of such systems based on HgCdTe lags far behind the corresponding level of development of systems based on A^3B^5 and Ge/Si systems (Yakimov et al. 2017; Baril et al. 2015). The electron and hole spectra in the HgCdTe/HgTe/HgCdTe quantum wells have not been studied to date, and intensive studies are carried out in this direction (Kernreiter et al. 2016; Kozlov et al. 2016). One of the methods for investigating low-dimensional objects is the measurement of the admittance of structures involving quantum wells, superlattices, or quantum dot arrays (Brounkov et al. 1995; Zubkov et al. 2014; Izhnin et al. 2017). A convenient tool for characterizing the properties of the semiconductor near-surface layer is the metal–insulator–semiconductor (MIS) structure based on this material. In the future, studies of MIS structures based on HgCdTe with single quantum wells (SQW) may lead to the development of new types of multicolor detectors (Dvoretsky et al. 2010). However, there are still few studies on the properties of MIS structures based on HgCdTe with an inhomogeneous thickness distribution of the component composition of CdTe. In (Izhnin et al. 2016), the electrical characteristics of MIS structures based on MBE p-HgCdTe with the 5.6 nm-thick HgTe SQW were investigated.

The aim of this paper is to investigate the effect of the presence of 6.5 nm-thick HgTe SQW on the electrical properties of MIS structures based on $n(p)$-$Hg_{1-x}Cd_xTe$

✉ I. I. Izhnin
i.izhnin@carat.electron.ua

1 Scientific Research Company “Carat”, Stryjska 202, Lviv 79031, Ukraine

2 National Research Tomsk State University, Lenina 36, Tomsk 634050, Russia

3 A.V. Rzhanov Institute of Semiconductor Physics SB RAS, Ac. Lavrent`eva 13, Novosibirsk 630090, Russia

($x = 0.65$–0.71) with CdTe/Al_2O_3 insulator over a wide range of measurement conditions.

Methods

Test MIS structures were created on the basis of $Hg_{1-x}Cd_xTe$ grown by the MBE method on GaAs (013) substrates in the Rzhanov Institute of Semiconductor Physics of the Siberian Branch of the RAS, Novosibirsk. Structures based on *p*-HgCdTe (Nos. 1 and 3) and *n*-HgCdTe (No. 2) with HgTe SQWs were studied. The quantum well thickness is less than the critical thickness of the transition between normal and inverted band structures at low temperatures (Germanenko et al. 2013; Sengupta et al. 2013) for sample No. 1 and is close to the critical thickness for structures Nos. 2 and 3. For comparison, the electrophysical characteristics of MIS structures on the basis of a homogeneous composition of the *n*-HgCdTe film (No. 4, the composition is close to the composition of the barrier layers Nos. 1–3) and *n*-HgCdTe films with a near-surface graded-gap layer with a high CdTe content (No. 5) were also measured. The thickness of the graded-gap layer was 0.5 µm, and the composition on the film surface is close to 0.43. Some technological parameters of the investigated MIS structures are shown in Table 1.

The low-temperature Al_2O_3 insulator layers formed by atomic-layer deposition (ALD) with the thickness of about 70 nm were used. For structures Nos. 1–4, between the ALD Al_2O_3 layer and the upper barrier layer, the 40 nm-thick CdTe buffer layer was grown in the MBE process. At the top of the ALD Al_2O_3 layer, indium electrodes with the area of about 0.155 mm^2 were formed. Figure 1a shows schematically the location of layers in the SQW structures Nos. 1–3. Figure 1b shows the distribution of the CdTe content over the $Hg_{1-x}Cd_xTe$ film (structure No. 2) in the SQW region measured with an automatic ellipsometer. The barrier layers had regions doped with indium (Fig. 1b, points show the boundaries of these regions).

The measurements were carried out with an automated setup for admittance spectroscopy of nanoheterostructures based on the Janis non-optic cryostat and the Agilent E4980A immittance meter. For the forward direction of the voltage sweep, measurements were made with the change of the bias voltage from negative values to positive ones, and in the reverse direction of the voltage sweep—from positive to negative ones.

Table 1 Technological parameters of MIS structures

No.	SQW parameters			Conductivity type	Insulator type
	Buffer layer parameters		Well thickness, nm		
	CdTe content	Thickness, nm			
1	0.65	35	5.6	*p*	CdTe/Al_2O_3
2	0.71	30	6.5	*n*	CdTe/Al_2O_3
3	0.65	30	6.5	*p*	CdTe/Al_2O_3
4	Without SQW and graded-gap layer, $x = 0.72$			*n*	CdTe/Al_2O_3
5	Without SQW, with graded-gap layer, $x = 0.23$			*n*	Al_2O_3

Results and discussion

Figure 2 shows the capacitance–voltage (*C*–*V*) characteristics of the MIS structure No. 1 measured at different frequencies at the temperature of 9 K for the forward voltage sweep. For *C*–*V* curves of the MIS structure based on *p*-HgCdTe with the SQW thickness of 5.6 nm, there is a complicated picture of the capacitive maxima in the strong inversion mode associated with the recharge of the quantum well levels when the voltage bias changes. The electrical characteristics of a similar MIS structure are considered in more detail in Izhnin et al. (2016). It can be noted that the maxima at the temperature of 9 K are observed at

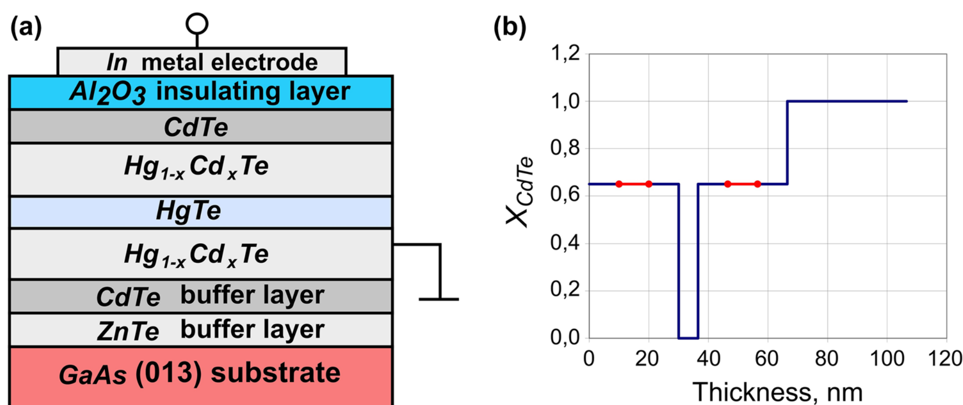

Fig. 1 Schematic representation of HgCdTe MIS structures Nos. 1–3 with HgTe SQW (**a**) and distribution of CdTe content over the film thickness in SQW region for structure No. 2 (**b**)

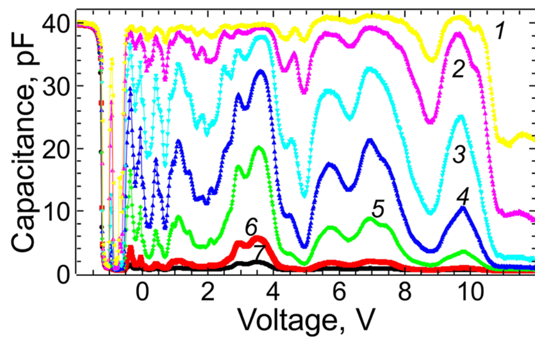

Fig. 2 *C–V* characteristics of structure No. 1 based on *p*-HgCdTe with an SQW measured at the temperature of 9 K for various frequencies, kHz: *1*—1, *2*—2, *3*—5, *4*—10, *5*—20, *6*—50, and *7*—100

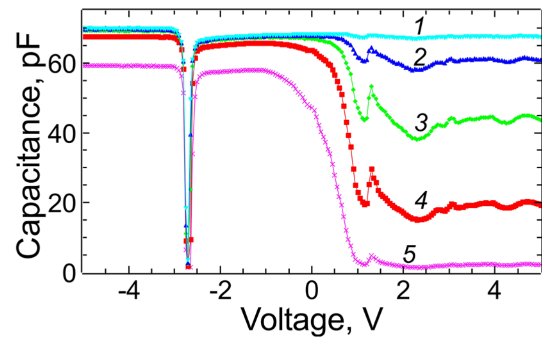

Fig. 4 *C–V* characteristics of structure No. 3 based on *p*-HgCdTe with an SQW measured at the temperature of 8 K for various frequencies, kHz: *1*—2, *2*—5, *3*—10, *4*—20, and *5*—50

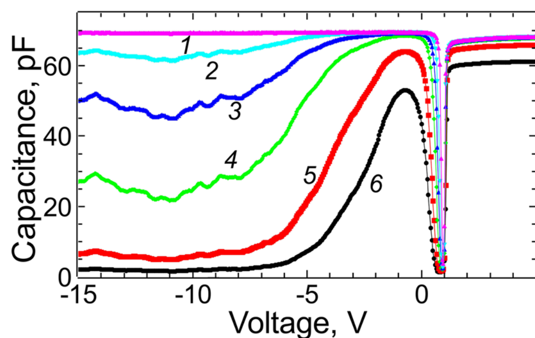

Fig. 3 *C–V* characteristics of structure No. 2 based on *n*-HgCdTe with an SQW measured at the temperature of 8 K for various frequencies, kHz: *1*—10, *2*—50, *3*—100, *4*—200, *5*—500, and *6*—1000

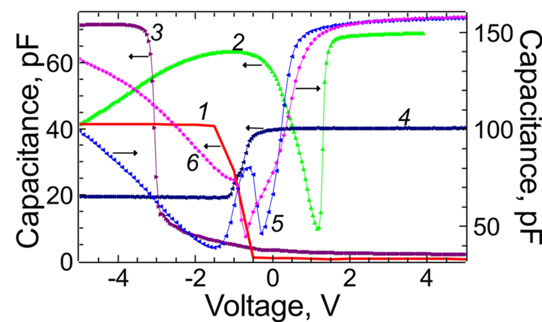

Fig. 5 *C–V* characteristics of structures based on HgCdTe measured at the frequency of 50 kHz and temperatures of 8 (*5*) and 77 K (*1–4*, *6*) for various samples, No.: *1*—1, *2*—2, *3*—3, *4*—4, and *5*, *6*—5

frequencies not exceeding 100 kHz, and almost disappear when the structure is heated to 77 K.

Figure 3 shows the *C–V* characteristics of the structure No. 2 based on *n*-HgCdTe with the SQW thickness of 6.5 nm measured at 8 K for the reverse voltage sweep. A decrease in capacitance at the frequency of 1 MHz in the accumulation mode is due to the effect of the series resistance of the film bulk on the measured capacitance. An unusual feature of *C–V* curves is the capacitance maximum at the beginning of the strong inversion. The wide maximum at the beginning of the strong inversion decreases with increase in temperature. At voltages from − 15 to − 7 V, weak non-monotonicity is observed on the *C–V* curve.

Figure 4 shows the *C–V* characteristics of the structure No. 3 based on *p*-HgCdTe with the SQW of 6.5 nm thickness measured at 8 K for the forward voltage sweep. A maximum at the beginning of a strong inversion is also observed for this structure, as well as non-monotonicity at voltages from 1 to 5 V. Figure 5 shows the *C–V* curves of the investigated MIS structures at 77 K. Capacitive maxima for structures with SQW (Nos. 1–3) at 77 K are less pronounced, and the *C–V* characteristic of the reference sample No. 4 does not show maxima and has a high-frequency appearance at frequencies from 1 kHz. The *C–V* structure based on the graded-gap *n*-HgCdTe No. 5 at the temperature of 8 K has maxima associated with the recharging of deep levels, which become less pronounced at the temperature of 77 K.

For the studied structures, the concentrations of the majority charge carriers were determined from capacitive measurements (Table 2). In addition, the values of the series resistance of the epitaxial film bulk (R_{bulk}) as well as the product of the area of the structure (A) and the differential resistance of the space-charge region (R_{scr}) in a strong inversion mode ($R_{scr}A$) were found at the temperatures of 8 and 77 K. Equivalent circuits of the MIS structure in different modes and the methods used are described in Voitsekhovskii et al. (2014, 2017a). For structures with SQWs, small values of the $R_{scr}A$ product are determined (compared with the values of this parameter for structure No. 4 without SQW). The increase in the values of the $R_{scr}A$ product upon heating from 8 to 77 K, which is observed for structures Nos. 1–3, 5, is not typical (Voitsekhovskii et al. 2015, 2017b). For these structures, the $R_{scr}A$ values in the maxima on the *C–V* curves

Table 2 Parameters of MIS structures determined from the admittance measurements

No.	Majority charge carrier concentration, cm^{-3}	R_{bulk} at 200 kHz, kΩ		$R_{scr}A$ in far strong inversion mode at 100 kHz, Ω cm^2		$R_{scr}A$ in capacitive maxima at 100 kHz, Ω cm^2	
		77 K	8 K	77 K	8 K	77 K	8 K
1	1.2×10^{12}	35.8	10.0	2929	4510	1674	321
2	1.1×10^{13}	66.2	16.8	96	22	23	2
3	2.3×10^{12}	86.5	44.2	300	332	181	5
4	3.0×10^{15}	6.2	4.1	18,700	25,300	–	–
5	6.7×10^{14}	0.3	0.2	11	39	5	3

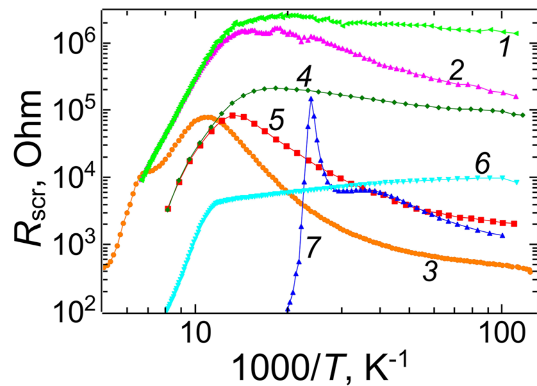

Fig. 6 Temperature dependencies of differential resistance of SCR measured at the frequency of 200 kHz for far strong inversion mode (*1*, *4*, *6*) and voltage corresponding to capacitive maximum (*2*, *3*, *5*, *7*) for various structures, No: *1*, *2*—1, *3*—2, *4*, *5*—3, and *6*, *7*—5

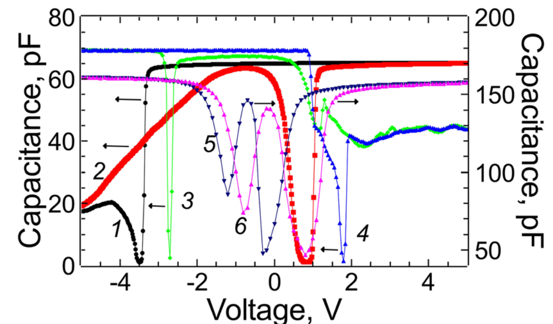

Fig. 7 *C–V* characteristics of structures based on HgCdTe measured at the frequencies of 2 (*5*, *6*), 10 (*3*, *4*), 500 (*1*, *2*) kHz and temperature of 8 K at forward (1, 3, 5) and reverse (2, 4, 6) voltage sweeps for various samples, No.: *1, 2*—2, *3, 4*—3, and *5, 6*—5

are smaller than in the mode of a far strong inversion, which is associated with a higher rate of generation of minority charge carriers at the voltages corresponding to the maxima.

Figure 6 shows the dependencies of the differential resistance R_{scr} for the studied samples on the reciprocal temperature at bias voltages corresponding to the capacitive maximum at the beginning of a strong inversion, as well as in the far strong inversion mode. Figure 6 shows that, at voltages corresponding to maxima in the *C–V* characteristic, the differential resistance of structures with SQWs increases when the sample is heated from 8 K. This results in a higher frequency appearance of *C–V* characteristics at a higher temperature, which is not typical for structures without SQW. The high-temperature drop for structures with SQWs cannot be explained by the diffusion processes of minority charge carriers from the quasi-neutral bulk, since the diffusion drop for the composition $x=0.65–0.71$ should occur at significantly higher temperatures. For structure No. 5, which has deep levels in the graded-gap layer, the differential resistance at the capacitive maximum (curve 7) also increases when heated from 8 K, and in the far strong inversion, there is a form of the dependence $R_{scr}(1/T)$ (curve 6) characteristic of most MIS structures based on $Hg_{1-x}Cd_xTe$ with the composition $x=0.22–0.23$ (Voitsekhovskii et al. 2015). The maxima on the *C–V* characteristics of structures with SQWs or with deep levels are associated with the appearance of additional generation current of minority charge carriers at the corresponding voltages. This current for structures Nos. 1–3 is due to the emission of minority carriers from SQW, and that for structure No. 5 is associated with generation via deep levels.

Figure 7 shows the *C–V* characteristics of MIS structures based on HgCdTe with SQW (as well as with deep levels) for different directions of bias voltage sweeps. The shift of the *C–V* curves along the voltage axis when changing the direction of the sweep is caused by hysteresis phenomena (Voitsekhovskii et al. 2018). For structures with SQW, the change in the direction of the sweep leads to a significant change in the amplitude and width of the maximum on the *C–V* characteristics. When the voltage corresponding to a far strong inversion is applied to the structure, minority charge carriers immediately escape from the well, so the maximum at *C–V* curves under these conditions does not manifest itself (curves 1 and 4). In the case of the presence of deep levels in the space-charge region (SCR) (structure No. 5), a change in the direction of the sweep does not significantly affect the amplitude and width of the capacitive maximum (curves 5 and 6).

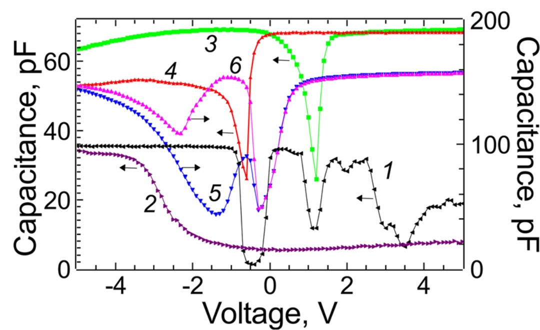

Fig. 8 *C–V* characteristics measured at the temperatures of 8 (*1*, *2*, *5*, *6*) and 77 (*3*, *4*) K and frequencies of 2 (*1*, *2*, *5*, *6*) and 20 (*3*, *4*) kHz in dark mode (*1*, *3*, *5*) and at LED illumination (*2*, *4*, *6*) for various samples, No: *1, 2*—1, *3, 4*—2, and *5*, *6*—5

Figure 8 shows the *C–V* characteristics of the MIS structures Nos. 1, 2, 5, measured in the dark mode, as well as when illuminated with radiation with a wavelength of 0.94 µm. From Fig. 8 it is clear that, for illuminated structures with SQWs, capacitive maxima almost disappear, and for a structure with deep levels, the maximum becomes more pronounced (its amplitude and width increase). The difference in the nature of the influence of radiation on the *C–V* curves is determined by the difference in the mechanisms of formation of capacitive maxima in the presence of SQW and deep levels in the active region. Under illumination, minority charge carriers are ejected from SQW due to photoexcitation; therefore, the escape of charge carriers at the beginning of a strong inversion does not occur (the well is already empty). In the case of the presence of deep levels in the SCR, illumination leads to an increase in the concentrations of mobile charge carriers, which leads to more intense generation–recombination via deep levels.

It is most likely that, in the dark mode, there are two mechanisms for the ejection of charge carriers from the quantum well due to thermal excitation, as well as through tunneling processes. Then, a wide maximum on the *C–V* curve is associated with tunnel transitions, which is confirmed by the type of temperature dependence of the differential resistance, and non-monotonicity in a far strong inversion mode with thermal emission of carriers from the SQW. More pronounced non-monotonicities for the *p*-HgCdTe-based structure with SQW (as compared to the No. 2 structure based on *n*-HgCdTe) are associated with the effects of degeneracy and non-parabolicity of the conduction band (Izhnin et al. 2016). The high-temperature drop of the differential resistance (at temperatures of about 100 K) is probably due to the thermal emission of carriers from the SQW. The mechanism of the occurrence of a wide maximum in the *C–V* curves for structures Nos. 2 and 3 is confirmed by measurements of the capacitance dependencies under illumination, as well as at different directions of voltage sweep.

The differences in the *C–V* characteristics in strong inversion for structures based on *p*-HgCdTe (Nos. 1 and 3) can be determined by the thickness of the quantum well, since, with a thickness of 5.6 nm, the correct band structure is characteristic, and with a thickness of 6.5 nm, the semiconductor is close to gapless.

Conclusions

For the first time, the admittance of MIS structures based on *n*(*p*)-$Hg_{1-x}Cd_xTe$ ($x = 0.65$–0.71) with HgTe SQWs in the active region has been experimentally investigated in a wide range of temperatures, frequencies, and voltages. It is established that the electrical characteristics of the structures studied are largely determined by the presence of the quantum well. The *C–V* characteristics of MIS structures based on *p*-HgCdTe with SQW with a thickness of 5.6 nm show pronounced maxima in the strong inversion mode at low temperatures, which are associated with the recharging of quantization levels in SQW. The capacitive dependencies of MIS structures based on *n*(*p*)-HgCdTe with SQW with a thickness of 6.5 nm are characterized by a wide maximum at the beginning of a strong inversion, which is associated with the emission of minority charge carriers from SQW by tunneling. Identified features allow us to associate the occurrence of these maxima with charge carrier ejection from the SQW.

Compliance with ethical standards

Conflict of interests The authors declare that they have no conflict of interests.

References

Baril N, Bandara S, Hoeglund L, Henry N, Brown A, Billman C, Maloney P, Nallon E, Tidrow M, Pellegrino J (2015) Low operating bias InAs/GaSb strain layer superlattice LWIR detector. Infrared Phys Technol 70:58–61

Benyahia D, Martyniuk P, Kopytko M, Antoszewski J, Gawron W, Madejczyk P, Rutkowski J, Gu P, Faraone L (2016) nBn HgCdTe infrared detector with HgTe (HgCdTe)/CdTe SLs barrier. Opt Quantum Electron 48:215

Brounkov PN, Benyattou T, Guillot G, Clark SA (1995) Admittance spectroscopy of InAlAs/InGaAs single-quantum-well structure with high concentration of electron traps in InAlAs layers. J Appl Phys 77:240–243

Dvoretsky S, Mikhailov N, Sidorov Y, Shvets V, Danilov S, Wittman B, Ganichev S (2010) Growth of HgTe quantum wells for IR to THz detectors. J Electron Mater 39:918–923

Germanenko AV, Minkov GM, Rut OE, Sherstobitov AA, Dvoretsky SA, Mikhailov NN (2013) Two-dimensional semimetal in wide HgTe quantum wells: charge-carrier energy spectrum and magnetotransport. Semiconductors 47:1562–1566

Izhnin II, Nesmelov SN, Dzyadukh SM, Voitsekhovskii AV, Gorn DI, Dvoretsky SA, Mikhailov NN (2016) Admittance investigation of MIS structures with HgTe-based single quantum wells. Nanoscale Res Lett 11:53

Izhnin II, Fitsych OI, Pishchagin AA, Kokhanenko AP, Voitsekhovskii AV, Dzyadukh SM, Nikiforov AI (2017) Temperature spectra of conductance of Ge/Si pin structures with Ge quantum dots. Nanoscale Res Lett 12:131

Kernreiter T, Governale M, Zlicke U (2016) Quantum capacitance of an HgTe quantum well as an indicator of the topological phase. Phys Rev B 93:241304

Kozlov DA, Savchenko ML, Ziegler J, Kvon ZD, Mikhailov NN, Dvoretskii SA, Weiss D (2016) Capacitance spectroscopy of a system of gapless Dirac fermions in a HgTe quantum well. JETP Lett 104:859–863

Selamet Y, Zhou YD, Zhao J, Chang Y, Becker CR, Ashokan R, Grein CH, Sivananthan S (2004) HgTe/HgCdTe superlattices grown on CdTe/Si by molecular beam epitaxy for infrared detection. J Electron Mater 33:503–508

Sengupta P, Kubis T, Tan Y, Povolotskyi M, Klimeck G (2013) Design principles for HgTe based topological insulator devices. J Appl Phys 114:043702

Voitsekhovskii A, Nesmelov S, Dzyadukh S (2014) Influence of composition of the near-surface graded-gap layer on the admittance of metal-insulator-semiconductor structures based on graded-gap MBE n-$Hg_{1-x}Cd_xTe$ in wide temperature range. Opto-Electron Rev 22:236–244

Voitsekhovskii AV, Nesmelov SN, Dzyadukh SM, Vasil'ev VV, Varavin VS, Dvoretsky SA, Mikhailov NN, Yakushev MV (2015) Admittance of metal–insulator–semiconductor structures based on graded-gap HgCdTe grown by molecular-beam epitaxy on GaAs substrates. Infrared Phys Technol 71:236–241

Voitsekhovskii AV, Nesmelov SN, Dzyadukh SM (2017a) Admittance measurements in the temperature range (8 – 77) K for characterization of MIS structures based on MBE n-$Hg_{0.78}Cd_{0.22}Te$ with and without graded-gap layers. J Phys Chem Solids 102:42–48

Voitsekhovskii AV, Nesmelov SN, Dzyadukh SM, Varavin VS, Dvoretskii SA, Mikhailov NN, Yakushev MV, Sidorov GY (2017b) Electrical characterizations of MIS structures based on variable-gap n(p)-HgCdTe grown by MBE on Si(013) substrates. Infrared Phys Technol 87:129–133

Voitsekhovskii AV, Nesmelov SN, Dzyadukh SM, Varavin VS, Dvoretskii SA, Mikhailov NN, Yakushev MV, Sidorov GY (2018) Electrical characterization of insulator-semiconductor systems based on graded band gap MBE HgCdTe with atomic layer deposited Al_2O_3 films for infrared detector passivation. Vacuum 158:136–140

Yakimov AI, Kirienko VV, Bloshkin AA, Armbrister VA, Dvurechenskii AV (2017) Plasmon polariton enhanced mid-infrared photodetectors based on Ge quantum dots in Si. J Appl Phys 122:133101

Zubkov VI, Yakovlev IN, Litvinov VG, Ermachihin AV, Kucherova OV, Cherkasova VN (2014) Analysis of the electrostatic interaction of charges in multiple InGaAs/GaAs quantum wells by admittance-spectroscopy methods. Semiconductors 48:917–923

Publisher's Note Springer Nature remains neutral with regard to jurisdictional claims in published maps and institutional affiliations.